DD proton spectrum for diagnosing the areal density of imploded capsules on Shenguang III prototype laser facility*

Teng Jian(滕 建), Zhang Tian-Kui(张天奎), Wu Bo(伍 波), Pu Yu-Dong(蒲昱东), Hong Wei(洪 伟), Shan Lian-Qiang(单连强), Zhu Bin(朱 斌), He Wei-Hua(何卫华), Lu Feng(卢 峰), Wen Xian-Lun(温贤伦), Zhou Wei-Min(周维民), Cao Lei-Feng(曹磊峰), Jiang Shao-En(江少恩), and Gu Yu-Qiu(谷渝秋)†

Science and Technology on Plasma Physics Laboratory, Laser Fusion Research Center, China Academy of Engineering Physics, Mianyang 621900, *China*

(Received 9 October 2013; revised manuscript received 21 January 2014; published online 15 May 2014)

The primary DD proton spectrum is used for diagnosing the fuel-shell areal density ρR of imploded capsules on Shenguang III (SG-III) prototype laser facility for the first time. A charged particle spectrometer (CPS) with a CR39 nuclear track detector is used to measure the DD proton spectrum. The proton spectrum is determined from both the proton track and its size. A typical proton energy peak shift from 3.02 MeV to 2.6 MeV is observed in our experiment, which yields a maximum ρR larger than 6 mg/cm^2.

Keywords: DD proton spectrum, charged particle spectrometer, areal density, implosion

PACS: 52.57.Fg, 52.70.Nc, 29.30.Ep **DOI:** 10.1088/1674-1056/23/7/075207

1. Introduction

In inertial confinement fusion (ICF) experiments, attaining the ignition requires the capsule to be symmetrically compressed[1,2] to achieve a high density and a high temperature. To character the compression feature of the capsule, the areal density ρR is often used to indicate the compression degree. It is probable to realize the ignition only when ρR is more than 0.4 g/cm^2 according to the Lawson criteria. The ρR is also strongly influences the degree of self-heating, the fractional burn, and the breakeven requirements.[3,4] It is critical to measure this quantity experimentally. Several methods have been proposed, among which the measurement of the energy peak shift of DD produced protons by a charged particle spectrometer (CPS) is an important one due to the close relationship between the compressed fuel and the particle spectral characteristics. It has been widely used to diagnose the areal density at several large laser facilities.[5–10] In Shenguang III (SG-III) prototype laser facility, the secondary neutron yield ratio method has been used to diagnose the areal density under a low density condition,[11] however an accurate measurement of the yield is necessary. The proton spectrometry method does not require any absolute number of the emitted protons (only their energy peak shifts are required) and is expected to be used in our experiment.

As the energy of the DD proton is only about 3 MeV, the protons from the ablated plasma (always have velocities larger than 10^7 cm/s) will interfere the DD proton spectrum measurements when ρR is large enough to bring on a large proton energy downshift. Usually, D^{3}He protons[7] and DD secondary protons[6] are more suitable for the diagnosis of ρR due to their higher energies. However, for the limited energy on Shenguang III prototype laser facility, the total number of DD secondary protons (^{3}He [< 0.82 MeV] +D$\rightarrow \alpha$ [1.7–6.6 MeV] + p* [12.6–17.5 MeV]) in DD implosion experiments is too low to give a spectrum. Fortunately, the imploded DD fuel density in our experiments is not so high that the maximum primary proton energy downshift is larger than 1.0 MeV, far higher than the energy of the protons from the plasma expansion. The protons produced in the laser plasma interaction have a maximum cutoff energy $E_{\max} = 3.51 \times 10^{-6}(I\lambda^2)^{1/3}$.[12] In our experiments, the laser intensity is about 7.1×10^{14} W/cm^2 and the wavelength is 0.35 μm. If the laser is directly incident into the capsule, $E_{\max}$ is about 0.16 MeV. For the indirect-driven implosion, $E_{\max}$ is even low. These low energy protons will have no influence on the primary DD proton spectrum in our experiment. In this paper, the method and the results on the areal density measurement of an imploded DD target by using the energy peak shift of DD produced primary protons are described.

The paper is organized as follows. Section 2 describes the experiment setup, and gives information on the laser and the target. In Section 3, the calibration of the charge particle spectrometer and the CR39 detector are presented. In Section 4, the possible noises on the CR39 detector are analysis and characterized, which is very important for obtaining the proton spectrum. In Section 5, the proton spectrum is gained by distinguishing the proton track from the noise track. In Section 6, some analysis about the areal density is carried out. A summary is presented in Section 7.

*Project supported by the Foundation of Science and Technology on Plasma Physics Laboratory, China (Grant No. 9140C680302130C68243).

†Corresponding author. E-mail: yqgu@caep.ac.cn

© 2014 Chinese Physical Society and IOP Publishing Ltd

2. Experiment setup

The experiments were performed on SG-III laser prototype facility at Laser Fusion Research Center, China Academy of Engineering Physics. SG-III laser prototype facility is an 8-beam neodymium-doped phosphate glass laser capable of delivering 10 kJ frequency-tripled laser in 1–10 ns, which is designed for indirect laser fusion researches. Its 8 beams gather to the two polar with an incidence angle of 45° relative to the perpendicular axis. In our experiments, 8 laser beams with total energy of 8×900 J and flat top pulse duration of 1 ns were incident into a hohlraum (diameter 1100 μm, length 1800 μm) to produce X-ray. The wall thickness of the hohlraum was 27 μm. The X-ray was then irradiated on a 320 μm diameter CH micro balloon with 19 atm D_2 gas filled. The wall of the micro balloon was 20 μm. A hole of 250 μm×250 μm on the hohlraum wall was used for the diagnosis of the implosion protons. The laser beams were smoothed with CCP and focused to a spot about 400 μm in diameter. In order to obtain a more uniform irradiance, each beam was moved a small distance of 50 μm away from the polar sides to the equatorial plane. The average on-target laser intensity was $\sim 7.1\times10^{14}$ W/cm^2.

In the pure DD-filled target, the primary fusion reactions are

$$\mathrm{D}+\mathrm{D}\rightarrow{}^3\mathrm{He}(0.82\ \mathrm{MeV})+\mathrm{n}(2.45\ \mathrm{MeV}), \quad (1)$$

$$\mathrm{D}+\mathrm{D}\rightarrow\mathrm{T}(1.01\ \mathrm{MeV})+\mathrm{p}(3.02\ \mathrm{MeV}). \quad (2)$$

Spectra were observed by using a charged-particle spectrometer consisting of a 6.2 kG permanent magnet with CR-39 nuclear track-etch detectors. The detector was placed at 26° in south-east on the target chamber equatorial plane. A 5 μm Al filter was used to protect the CR-39 detector from the laser accelerated proton and other ablator heavy ions. The 0.82 MeV ^{3}He, which has a penetration depth of only 2.5 μm in Al, could not be detected by the CR39 detector. The 1.01 MeV tritium could enter the CR39 detector, however its track size is different from that of the 3 MeV protons.

3. Calibration of the charge particle spectrometer and the CR39 detector

The charge particle spectrometer and the CR39 detector were calibrated in the GIC4117 accelerator at Peking Normal University. This accelerator could produce protons with a current down to 30 pA and energy up to 3.4 MeV. The energy spread could be lower than 1%. The spot size was about 10 mm. The schematic diagram of the charged-particle spectrometer is shown in Fig. 1.

As the proton yield in the implosion experiment was low, a larger entrance aperture of 10 mm in length and 0.25 mm in width was used to collect enough protons. The proton detector was placed 5 cm behind the CPS. The relatively position between the CPS and the proton detector was fixed.

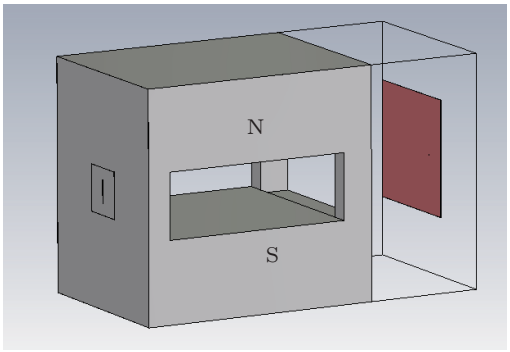


Fig. 1. (color online) Schematic diagram of the charged-particle spectrometer (CPS). A 6.2 kG quadrate dipole magnet, 10 cm in its longest dimension, disperses protons in the energy range 0.5–10 MeV according to the ratio of momentum to charge. A CR39 nuclear track detector is placed 5 cm behind the CPS.

The proton signal on the CR39 nuclear track detector could appear only after a series of processing, however, the radiochromic dosimeters film (RCF) could turn color immediately after the protons radiated. In the CPS calibration experiment, an RCF was used instead of CR39 to record the proton signals. By adjusting the energies of the protons, the real relationship between the proton energy and the transverse deflection distance on the CR39 nuclear track detector was deduced, which is shown in Fig. 2. This distance–energy relationship would be used in the implosion experiment to estimate the energy of the protons.

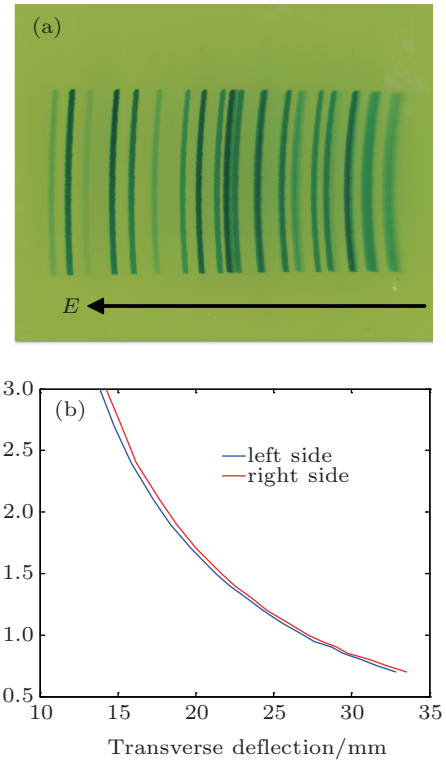


Fig. 2. (color online) The calibrated relationship between the proton energy and the transverse deflection distance on the detector. The effects of the slit width on the deflection distance are presented. (a) Original calibrated proton signal on RCF. The energy is higher at the left. (b) The energy–transverse deflection relationship obtained.

The gyro radius of a charged particle in a magnetic field is proportional to the particle's energy E through the relationship

$$R_{\text{gyro}} \propto \frac{\sqrt{AE}}{Z}, \tag{3}$$

where A is the atomic mass and Z is the atomic number.

The other heavy ions with the same value of $\sqrt{AE}/Z$ would also deposit at the same position of the protons. To prevent the influence of the other ions, the proton track on the CR39 detector was also calibrated. The relationship of the proton energy and the track diameter is presented in Fig. 3. The CR39 sheet was etched in a 6 mol/L NaOH solution (at temperature 60 °C) for 6 h. The other heavy ions at the same position on the RCF had very different track sizes from that of the protons.[7]

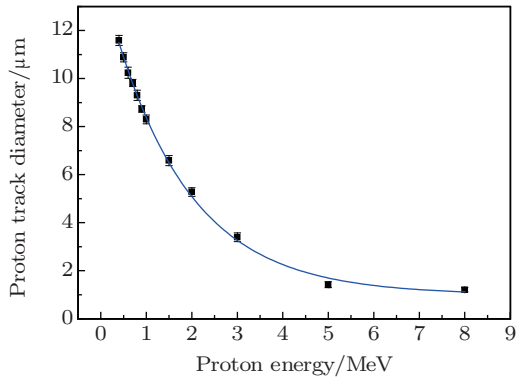


Fig. 3. (color online) Measured diameters of tracks in CR-39 for accelerator-generated protons with energies ranging from 0.4 MeV to 8 MeV. The solid line is the fitting curve, and the error bar is given by a random measure of several tracks.

4. Noise analysis

As the signal to noise ratio is very low in our experiment, an analysis of the noise is necessary. The TASLIMAGE system and the Color 3D Laser Microscope VK-9700K were used for the scanning and the analysis of the CR39 nuclear track detector. The noise could be produced before and after the experiment. Before the experiment, three different noises exist. The first noise is the dust on the surface, which is deduced by scanning several different CR39 sheets. The distributions of the track sizes are the same for all CR39 sheets and the number of the track will increase with time when the CR39 is exposed to air, which is seen in Table 1. The number density is about 10^4 cm^{-2}. This noise has a typical size of 3–5 μm, as shown in Fig. 4. The r_{min} is the short size of the track, and r_{max} is the long size of the track.

The second noise is the intrinsic noise caused by the radioactivity in the environment. The number density is from several tens cm^{-2} to several hundreds cm^{-2} for different CR39 sheets. The typical shape of this noise is shown in Fig. 5(a). It has an isotropic distribution and the track usually has a tail.

Table 1. Track number of the same CR39 at different time.

No. of files by scanning	Number of tracks	Scanning time
single1	53644	2013.5.24 a.m.
	clean	
single3	27359	
single4	20350	2013.5.24 p.m.
single5	26442	
single6	46422	2013.5.27 a.m.
single7	59783	2013.5.27 p.m

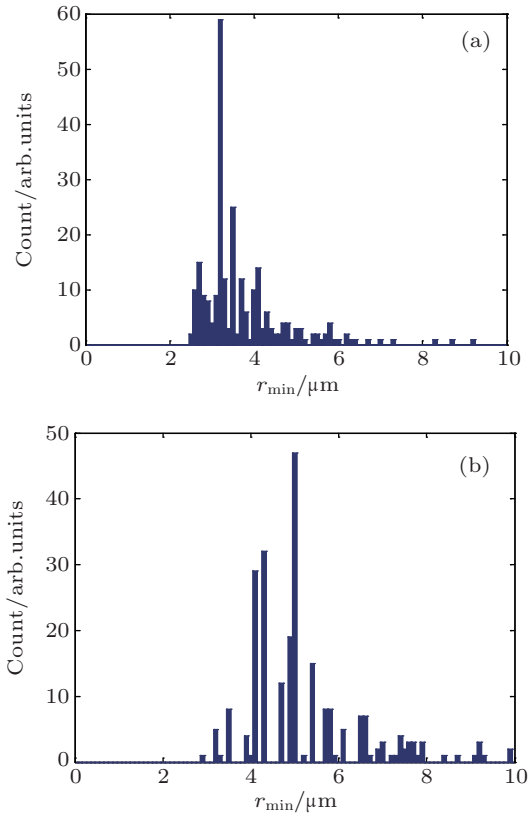


Fig. 4. (color online) Distributions of the track size: (a) short size, (b) long size.

The third noise is the defect, which has an irregularly size and can be expelled easily. To exclude these noises, the deepness of the protons track and the noise track was also measured by the Color 3D Laser Microscope VK-9700K, and the depth of the proton track was larger than that of the noise with the same track size.

During the experiment, some other noises could also be introduced. The first one is the T and ^{3}He ions produced in the DD reaction. A 5 μm thick Al foil before the CR39 detector can prevent the ^{3}He ions with energy lower than 0.82 MeV. The T ion can penetrate the 5 μm Al foil, but the track size is larger than that of the protons at the same deflected position.[7] The second noise is protons produced in the interaction of laser plasma, which has a maxim cutoff energy $E_{\text{max}} = 3.51 \times 10^{-6}(I\lambda^2)^{1/3}$. In our experiments, the laser intensity was about 7.1×10^{14} W/cm^2 and the wavelength was 0.35 μm. If the laser was directly incident into the capsule,

E_{max} was about 0.16 MeV. For the indirect-driven implosion, E_{max} was even low. These low energy protons would have no influence on the DD proton spectrum in our experiment. The third noise is the secondary neutron, which has a number of only 10^{-4} of the primary protons and can be ignored.

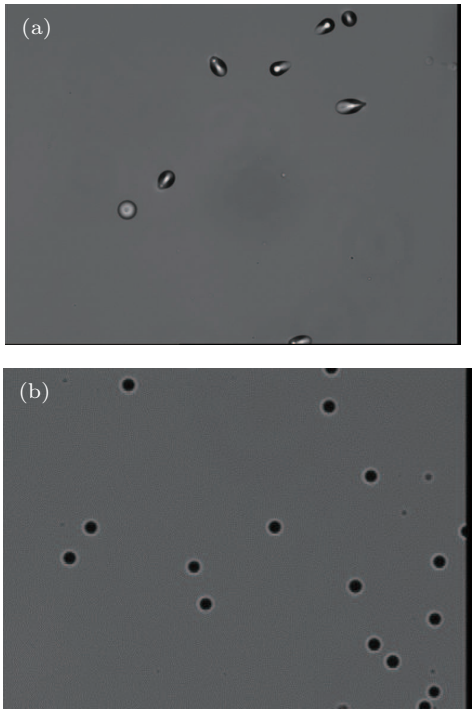


Fig. 5. The tracks of (a) the intrinsic noise by the radioactivity in the environment and (b) the proton signal.

5. The proton energy spectrum

As the TASLIMAGE system could only give the 2D image of the track and the size of the dusty was similar to that of the proton with energy between 2 MeV and 3 MeV, the experiment result was analyzed by the Color 3D Laser Microscope VK-9700K. The size and the depth of the track on the CR39 detector were measured. As the incidence angle on the CR39 was larger than 80°. The track with a tail was not considered as the proton track. The calibrated relationship of the proton energy and the transverse deflection distance was used to decide the proton energy at certain transverse position of the CR39 detector. The relationship of the proton energy and the track size was used to eliminate the influence of the other ions. The finally proton energy spectrum is shown in Fig. 6.

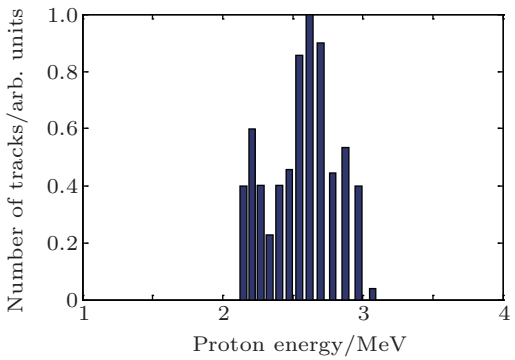


Fig. 6. (color online) The proton energy spectrum of the experiment.

6. Areal density of the imploded capsules

The stopping power of the test particle in a field of background particles is given as[13]

$$\frac{\mathrm{d}E^{\mathrm{t/f}}}{\mathrm{d}x} = -\frac{(Z_{\mathrm{t}}e)^2}{\upsilon_{\mathrm{t}}^2}\omega_{\mathrm{pf}}^2 G(x_{\mathrm{t/f}})\ln\Lambda_{\mathrm{b}}, \tag{4}$$

with

$$G(x_{\mathrm{t/f}}) = \mu(x_{\mathrm{t/f}}) - \frac{m_{\mathrm{f}}}{m_{\mathrm{t}}}\left\{\mu' - \frac{1}{\ln\Lambda_{\mathrm{b}}}[\mu+\mu']\right\}, \tag{5}$$

where $Z_{\mathrm{t}}e$ is the test particle charge; $\upsilon_{\mathrm{t}}(\upsilon_{\mathrm{f}})$ is the test (field) particle velocity with $x^{\mathrm{t/f}} = \upsilon_{\mathrm{t}}^2/\upsilon_{\mathrm{f}}^2$; m_{t} (m_{f}) is test (field) particle mass; $\omega_{\mathrm{pf}} = \sqrt{4\pi n_{\mathrm{f}} e_{\mathrm{f}}^2/m_{\mathrm{f}}}$ is the field plasma frequency; $\mu(x_{\mathrm{t/f}}) = 2\int_0^{x_{\mathrm{t/f}}} \mathrm{e}^{-\xi}\sqrt{\xi}\,\mathrm{d}\xi/\sqrt{\pi}$ is the Maxwell integral; $\ln\Lambda_{\mathrm{b}} = \ln(\lambda_{\mathrm{D}}/p_{\mathrm{min}})$, λ_{D} is the Debye length in the nodegenerate regime, $p_{\mathrm{min}} = \sqrt{p_\perp^2 + (\hbar/2m_{\mathrm{r}}u)^2}$; and $p_\perp = e_{\mathrm{t}}e_{\mathrm{f}}/m_{\mathrm{r}}u^2$ is the classical impact parameter for 90° scattering, with m_{r} the reduced mass and u the relative velocity. However, in the low temperature and high density regime, the electron quantum degeneracy effects must be considered in calculating λ_{D} and p_{min}, and the electron temperature must be replace by an effective temperature. On the contrary, the electron temperature can be used directly to calculate λ_{D} and p_{min}. To describe the transition between these two conditions, an interpolation formula given by Ichimaru[14] is used in our calculation. As the fuel has a relatively high temperature and a small ρR, most energy loss occurs in the low temperature high density shell, for which ρR is almost temperature insensitive.[15] The proton energy shift is about 400 keV in our experiment

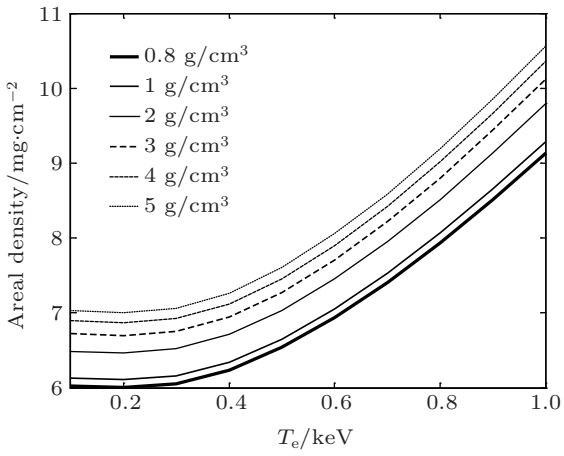


Fig. 7. The areal density at different shell plasma temperature and different density.

and the areal density at different shell plasma temperature and different density is shown in Fig. 7, from which we can see that the maximum ρR is larger than 6 mg/cm^2.

7. Summary

In summary, the primary DD proton spectrum has been used to measure the imploded fuel-shell areal density on Shenguang III prototype laser facility for the first time. The primary proton energy spectrum was observed using a charged-particle spectrometer consisting of a 6.2 kG permanent magnet with CR-39 nuclear track detectors. The CPS and the the CR39 nuclear track detector were calibrated in the GIC4117 accelerator at Peking Normal University before the experiment. The noise on the CR39 was analysis and characterized. From the measured spectrum, a typical peak energy shift from 3.02 MeV to 2.6 MeV was observed, which infers a maximum ρR larger than 6 mg/cm^2.

References

[1] Jing L F, Huang T X, Jiang S E, Chen B L, Pu Y D, Hu F and Cheng S B 2012 *Acta Phys. Sin.* **61** 105205 (in Chinese)

[2] Jiang S E, Miao W Y and Kuang L Y 2011 *Acta Phys. Sin.* **60** 055206 (in Chinese)

[3] Nuckolls J, Wood L, Theissen A and Zimmerman G 1972 *Nature* **293** 139

[4] Krokhin O N and Rozanov V B 1973 *Sov. J. Quantum Electron.* **2** 393

[5] Kitagawa Y, Tanaka K A, Nakai M, Yamanaka T, Nishihara K, Azechi H, Miyanaga N, Norimatsu T, Kanabe T, Chen C, Richard A, Sato M, Furukawa H and Nakai S 1995 *Phys. Rev. Lett.* **75** 3130

[6] Seguin F H, Li C K, Frenje J A, Hicks D G, Green K M, Kurebayashi S, Soures J M, Meyerhofer D D, Glebov V Yu, Radha P B, Stoeck C, Roberts S, Sorce C, Sangster T C, Cable M D, Fletcher K and Padalino S 2002 *Phys. Plasmas* **9** 2725

[7] Petrasso R D, Frenje J A, Li C K, Seguin F H, Rygg J R, Schwartz B E, Kurebayashi S, Radha P B, Stoeckl C, Soures J M, Delettrez J, Glebov V Yu, Meyerhofer D D and Sangster T C 2003 *Phys. Rev. Lett.* **90** 095002

[8] Seguin F H, Frenje J A, Li C K, Hicks D G, Kurebayashi S, Rygg J R, Schwartz B E, Petrasso R D, Roberts S, Soures J M, Meyerhofer D D, Sangster T C, Knauer J P, Sorce C, Glebov V Yu, Stoeck C, Phillips T W, Leeper R J, Fletcher K and Padalino S 2003 *Rev. Sci. Instrum.* **74** 975

[9] Frenje J A, Li C K, Rygg J R, Séguin F H, Casey D T, Petrasso R D, Delettrez J, Glebov V Yu, Sangster T C, Landen O and Hatchett S 2009 *Phys. Plasmas* **16** 022702

[10] Zylstra A B, Frenje J A, Séguin F H, *et al*. 2012 *Rev. Sci. Instrum.* **83** 10D901

[11] Kang X T, Chen J B, Deng C B, Liu Z J, Zhan X Y and Chen M 2008 *Rev. Sci. Instrum.* **79** 086109

[12] Hicks D G, Li C K, Seguin F H, Schnittman J D, Ram A K, Frenje J A, Petrasso R D, Soures J M, Meyerhofer D D, Roberts S, Sorce C, Stockl C, Sangster T C and Phillips T W 2001 *Phys. Plasmas* **8** 606

[13] Li C K and Petrasso R D 1995 *Phys. Plasmas* **2** 2460

[14] Ichimaru S 1994 *Statistical Plasma Physics* Vol. II (Reading: Addison-Wesley Publishing Company)

[15] Li C K, Hicks D G, Seǵuin F H, Frenje J A, Petrasso R D, Soures J M, Radha P B, Glebov Yu V, Stoeckl C, Harding D R, Knauer J P, Kremens R, Marshall F J, Meyerhofer D D, Skupsky S, Roberts S, Sorce C, Sangster T C, Phillips T W, Cable M D and Leeper R J 2000 *Phys. Plasmas* **7** 2578